

Analysis of Wave-Aberration by Use of the Wavelet Transform

Jin-Yi Sheu^{1,2}, Rong-Seng Chang¹, Ching-Huang Lin^{1,3}, and Ping-Lin Fan^{1,2}

¹*Institute of Optical Sciences, National Central University, Chung-Li, Taiwan 320, R.O.C.*

²*Department of Electric Engineering, Kwang Wu Institute of Technology,
151, I-Te St, Peitou, Taipei, Taiwan 112, R.O.C*

³*Department of Chemical Engineering, Hua Hsia College of Technology and Commerce,
111, Hwa-Hsin St, Chung Ho, Taipei, Taiwan 235, R.O.C.*

(Received August 28, 2001)

This work discusses the application of the wavelet transform technique for determining the wave aberration coefficients of a rotationally symmetric optical system. The proposed technique is used for polynomial fitting in data analysis. From the numerical example provided, our proposed method is shown to improve the numerical accuracy of the aberration coefficients deduced from the measured data of wave front deformations. Compared with the least-squares matrix inversion method, its performance is more stable under the input of Gaussian white noise. Simulation results are shown for both spherical aberration and defocusing.

PACS. 42.15.Dp – Wave fronts and ray tracing.

PACS. 42.15.Fr – Aberrations.

I. Introduction

A polynomial representation of the optical wave-front is essential in the analysis of interferometric test data and optical system performance. In many cases, an aberrated wave-front can be described by a few coefficients multiplying the terms of a well-chosen polynomial, such as the Zernike polynomials or the Seidel polynomials [1, 2, 3]; some of Zernike modes are related to classical primary aberrations. The Zernike coefficients can be estimated by the least-squares matrix inversion method (LS) and Gram-Schmidt orthogonalization, and the numerical results from both techniques are almost identical [3, 4]. The classical LS method of determining the Zernike coefficients from a sampled wave-front with measurement noise have been found to be numerically unstable [4].

In recent years, the wavelet transform (WT) was found to be applicable to different tasks, such as pattern recognition, image compression, fractal aggregates and sound analysis [5, 6]. The WT is an important linear time-frequency (space-frequency) representation, which can represent a signal by its localization both in the time space and frequency planes [7-10]. In this paper, we apply the technique to estimate the rotationally symmetric aberration coefficients (spherical aberration and defocus) when the wave-front is expanded in terms of Seidel polynomials. To improve numerical accuracy performance, it is desirable to minimize the approximation error from the measured data of the wave front by the least square error criteria. In this way, we have a unique solution for the unknown wave aberration coefficients by solving linear simultaneous equations.

Our proposed method is illustrated for a simulated aberrated wave-front. The aberration coefficients are obtained by two methods (LS and WT), and the numerical results are compared.

TABLE I. Seidel polynomials in Cartesian Coordinates.

j	U(x; y)	meaning
1	x	tilt in x direction
2	y	tilt in y direction
3	$x^2 + y^2$	defocus
4	$x^2 + 3y^2$	astigmatism
5	$y(x^2 + y^2)$	coma
6	$(x^2 + y^2)^2$	spherical aberration

The spherical aberration coefficient and defocus are estimated by the LS method in Section 2. In Section 3 we use the WT technique to estimate the rotationally symmetric aberration coefficients. The comparison between the LS method and the WT method are described in Section 4, where results of the evaluation of the simulations are presented. The final results and conclusions are discussed in Section 5.

II. Computed aberration coefficients by the least-squares method

A particular case of representation for primary aberration is the expression given by Kingslake [11]:

$$W(x; y) = w_6(x^2 + y^2)^2 + w_5y(x^2 + y^2) + w_4(x^2 + 3y^2) + w_3(x^2 + y^2) + w_2y + w_1x; \quad (1)$$

where $(x; y)$ are the rectangular coordinates of any point in the exit pupil plane, w_6 , w_5 , w_4 , w_3 , w_2 , and w_1 are the aberration coefficients for spherical aberration, coma, astigmatism, defocus, tilt about the y axis, and tilt about the x axis, respectively.

The wave-front phase of a rotationally symmetric optical system can be represented by an expansion of Seidel polynomials (see Table I). Seidel polynomials (in polar coordinates) are not recommended as a basis for wave-front fitting in the case of a lateral shearing interferometry system and a Hartmann test system. The wave-front phase is presented in rectangular coordinates, rather than polar coordinates.

Using the Seidel polynomial expansion as shown in Table I, the rotationally symmetric wave-front phase can be expressed as

$$W(x; y)_i = \sum_{j=3;6}^M s_j U_j(x; y)_i \quad i = 1; 2; \dots; M; \quad (2)$$

where j is the number of the expansion term ($j = 3, 6$ for the rotationally symmetric optical system), M is the number of measurements, and W_i is the wave-front phase of the i th measurement. We

collect all phase values W_i into a single vector

$$W(x; y) = \begin{pmatrix} 0 \\ W(x; y)_1 \\ W(x; y)_2 \\ \vdots \\ W(x; y)_M \end{pmatrix} = \begin{pmatrix} 1 \\ C \\ C \\ \vdots \\ A \end{pmatrix} \quad (3)$$

With equation (2) and equation (3), the wave-front measurements become

$$\begin{aligned} W(x; y) &= \sum_{i=1}^M W(x; y)_i = \sum_{i=1}^M \sum_{j=3,6} s_j U_j(x; y)_i \\ &= \sum_{j=3,6} s_j \sum_{i=1}^M U_j(x; y)_i = \sum_{j=3,6} s_j U_j(x; y) \end{aligned} \quad (4)$$

Equation (4) may be written conveniently in a matrix form,

$$W = Us; \quad (5)$$

where

$$W = \begin{pmatrix} 0 \\ W(x; y)_1 \\ W(x; y)_2 \\ \vdots \\ W(x; y)_M \end{pmatrix} = \begin{pmatrix} 1 \\ C \\ C \\ \vdots \\ A \end{pmatrix}; \quad U = \begin{pmatrix} 2 & 3 \\ U_3(x; y)_1 & U_6(x; y)_1 \\ 6 & 7 \\ U_3(x; y)_2 & U_6(x; y)_2 \\ 6 & 7 \\ \vdots & \vdots \\ 4 & 5 \\ U_3(x; y)_M & U_6(x; y)_M \end{pmatrix}; \quad s = \begin{pmatrix} s_3 \\ s_6 \end{pmatrix}$$

In general equation (5) represents an determined system of equations, wherein there are more equations (M) than unknown expansion coefficients (s_j). These expansion coefficients can be computed by the LS method [3]; that is, one tries to minimize

$$\psi = \sum_{i=1}^M \left(\sum_{j=3,6} s_j U_j(x; y)_i - W_i \right)^2 \quad (6)$$

The resultant equation can be written in the familiar form

$$U^T Us = U^T W; \quad (7)$$

and the desired Seidel coefficients may be obtained directly by inversion:

$$s = (U^T U)^{-1} U^T W; \quad (8)$$

The rotationally symmetric aberration coefficients can be determined from the Seidel coefficients as

$$W_3 = S_3; \quad (9-1)$$

$$W_3 = S_6: \quad (9-2)$$

With knowledge of the Seidel coefficients, the defocus and spherical aberration coefficients are obtained by equation (9-1) and equation (9-2), respectively.

III. Computed aberration coefficients by the wavelet transform

The WT of a signal $f(x)$ is defined as

$$C(a; b) = \langle f; h_{a;b} \rangle = \int_{-\infty}^{\infty} f(x) \frac{1}{a} h\left(\frac{x-b}{a}\right) dx: \quad (10)$$

When the signal is sampled on a regular grid, equation (10) can be rewritten as

$$C(a; b) = \langle f; h_{a;b} \rangle = \sum_{i=1}^N f(i) h_{a;b}(i): \quad (11)$$

The parameters a and b are called the dilation (scale) and shift (translation) parameter, respectively, and h is the mother wavelet function. This transformation can be expressed mathematically as a correlation between the input function and a continuous set of scaled wavelet mother functions. As the dilation factor a increases (decreases), the low-frequency (high-frequency) features are displayed.

The wavelets must satisfy the admissible condition with zero means [11, 12], and they must have some regularity so that the WT is local both in the space and the frequency domains.

In the computer simulation, 65×65 uniform sampling points and a Mexican hat wavelet were used as the input wave-front and the analyzing wavelet filter, respectively. The Mexican hat wavelet was chosen because it is localized optimally in space and spatial-frequency domains [13].

The Mexican hat wavelet was first introduced by Gabor, it is the second derivative of the Gaussian function:

$$h(t) = (1 - t^2) \exp\left(-\frac{t^2}{2}\right): \quad (12)$$

It is even and real valued. The Fourier transform of the Mexican hat wavelet is

$$H(f) = 4\sqrt{2} f^2 \exp(-2\sqrt{2} f^2): \quad (13)$$

It is also even and real valued, as shown in Fig. 1.

In the rotationally symmetric optical system, consider the input wave-front $W(x; y) = S_3(x^2 + y^2) + S_6(x^2 + y^2)^2 = S_3 U_3(x; y) + S_6 U_6(x; y)$, and a measurement vector V , where

$$\begin{aligned} V &= [W(x; y)_1; W(x; y)_2; \dots; W(x; y)_n] \\ &= S_3 [U_3(x; y)_1; U_3(x; y)_2; \dots; U_3(x; y)_n] \\ &\quad + S_6 [U_6(x; y)_1; U_6(x; y)_2; \dots; U_6(x; y)_n] \\ &= S_3 V_3 + S_6 V_6: \end{aligned} \quad (14)$$

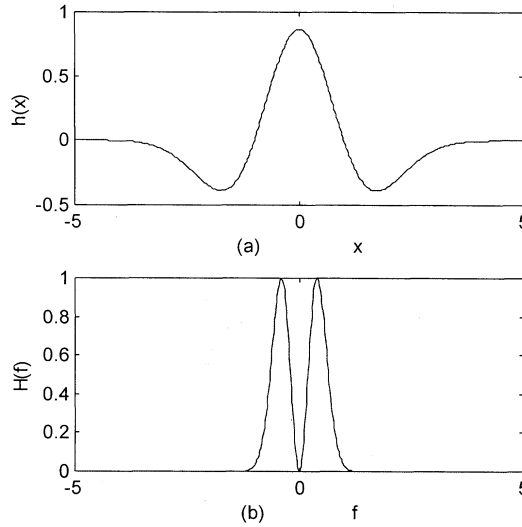


FIG. 1. (a) Mexican-hat wavelet $h(x)$ and (b) its Fourier spectrum $H(f)$.

By substitution of equation (14) in equation (11), the WT of the measurement vector can be expressed as follow:

$$\begin{aligned}
 C(a; b) &= \langle V; h_{a;b} \rangle = s_3 \langle V_3; h_{a;b} \rangle + s_6 \langle V_6; h_{a;b} \rangle \\
 &= s_3 \sum_{i=1}^3 V_3(i)h_{a;b}(i) + s_6 \sum_{i=1}^3 V_6(i)h_{a;b}(i) \\
 &= s_3 C_3(a; b) + s_6 C_6(a; b);
 \end{aligned}
 \tag{15}$$

The form of equation (15) can be written as

$$\begin{pmatrix} 2 \\ 6 \\ 6 \\ 4 \end{pmatrix} \begin{pmatrix} C(a; 1) \\ C(a; 2) \\ \vdots \\ C(a; n) \end{pmatrix} = \begin{pmatrix} 3 \\ 7 \\ 7 \\ 5 \end{pmatrix} \begin{pmatrix} C_3(a; 1) \\ C_3(a; 2) \\ \vdots \\ C_3(a; n) \end{pmatrix} + \begin{pmatrix} 2 \\ 6 \\ 6 \\ 5 \end{pmatrix} \begin{pmatrix} C_6(a; 1) \\ C_6(a; 2) \\ \vdots \\ C_6(a; n) \end{pmatrix} \begin{pmatrix} s_3 \\ s_6 \end{pmatrix};
 \tag{16}$$

where $a \geq 0$, n is the number of sampling points.

The measured data of the wave front $W(x; y)$ has optical random noise that makes it difficult to evaluate the wave-aberration coefficients directly. In our approach an algebraic expression $\hat{W}(x; y)$ is fitted to the set of wave front measurements by a least-squares error method. The new form of wave front can be written as

$$\hat{W}(x; y) = s_3(x^2 + y^2) + s_6(x^2 + y^2)^2;
 \tag{17}$$

if e_i is the difference between the wave front i th measurement and its fitted value

$$e_i = \hat{W}(x; y)_i - W(x; y)_i;
 \tag{18}$$

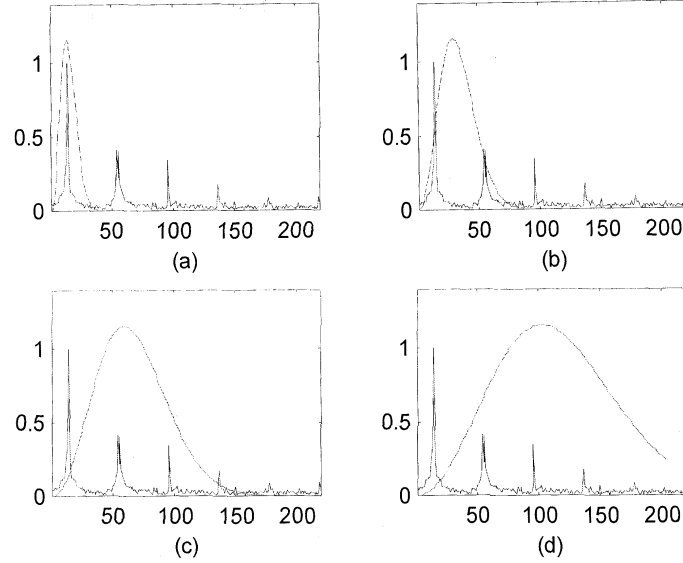


FIG. 2. Spectra of noisy signal (solid line) and Mexican-hat wavelet(dashed line) for dilation factor (a) $a = 3.2$, (b) $a = 1.4$, (c) $a = 0.7$, and (d) $a = 0.3$.
x (frequency); y (normalize frequency spectrum)

the sum of squares of the errors is denoted by

$$E = \sum_i (e_i)^2 \quad (19)$$

From equation (16) to equation (19), it is apparent that for a given suitable dilation factor a , the coefficients in the estimate $\hat{W}(x; y)$ are solved to minimize E .

IV. Computer simulation

In this paper, we try to estimate the defocus coefficient and spherical aberration coefficient by using the WT method and the LS method. The performance of the new wave-front estimate algorithm was tested by computer simulation. The simulation is also repeated for the LS algorithm for the purpose of comparison.

To test the method described above, we begin with the simple but very important case in which the corresponding simulated wave-front can be expressed as

$$W(x; y) = j \ 4:15(x^2 + y^2) + 3:55(x^2 + y^2)^2 + n(x; y); \quad (20)$$

the coefficients correspond to defocus and spherical aberration and are given in wavelength units, they are preset as $S_3 = j \ 4.15$ (defocus), $S_6 = 3.55$ (spherical aberration), and $n(x; y)$ is Gaussian white noise, the added Gaussian white noise is generated randomly.

In the test, the data are uniformly sampled over a 65×65 grid (4225 points in the unit square), and the noise mean and variance are preset as 0 and 0.41.

For the examples shown here, the aberration coefficients represented by the Seidel aberration coefficients are estimated both by the LS method and by the WT method, respectively. From equation (9-1) and equation (9-2), the W_3 (defocus) and W_6 (spherical) are determined. From equation (16) the defocus and spherical aberration coefficient can be computed by the WT method (given a suitable parameter a for the minimized E).

The frequency spectra of both the noisy wave-front and the Mexican hat wavelet for different dilations a are depicted in Fig. 2. Notice that in Fig. 2(a), the band-pass filter, which is the spectrum of the Mexican hat wavelet, blocks the high-frequency range, which is the spectra of the random noise. This spectrum is far beyond the cut-off window of the band-pass filter. The spectrum of random noise is broadly spreading, having less influence on the wavelet transform. In contrast to Fig. 2(a), the frequency filtering window of Figs. 2(b)-2(d) covers the noise frequency dominate range, which may produce numerical error.

The results of our analysis of the test wave-front are listed in Table II, including the rms of the preset wave front and the estimate results of the two algorithms. As shown in Table II, before the noise was added, the wave-front estimated by the two algorithms is shown with high accuracy. The consistent results identify the correctness of the new algorithm. After the noise was introduced, the reduced coefficients have a slight difference from the preset ones of the new algorithm. The error of the reduced coefficients and the rms value of the estimated wave-front from the WT method is less than that of the LS method. The contour of the original wave-front and reconstructed wave-front by the two algorithms are depicted in Fig. 3. Fig. 3(a) is a contour plot of $W(x; y)$ which describes the true topography of the wave-front. The contour plot of the wave-front in Fig. 3(b) was calculated using the WT method, while the contour plot of the wave-front in Fig. 3(c) was found using the LS technique. The contour map found using the WT method agrees quite well with map computed by original wave-front. On the meridional section ($x = 0$), the original aberration function and reconstructed aberration function obtained by the two algorithms are depicted in Fig. 4, it is shown that the WT method provides a better results than the LS method, especially in the middle part of the wave-front.

The SNR was computed to quantify and compare the capability of the WT algorithm with the LS algorithm. The SNR was determined as follows:

$$\text{SNR} = 10 \log_{10}(E_s/E_N): \quad (21)$$

TABLE II. Results of computer simulation.

preset Seidel coefficients	free from noise		noise added	
	WT	LS	WT	LS
$S_3 = -4.15$	-4.14999	-4.14999	-4.08581	-3.82135
$S_6 = 3.55$	3.54999	3.54999	3.38177	3.25416
rms = 0.640	0.640	0.640	0.638	0.633

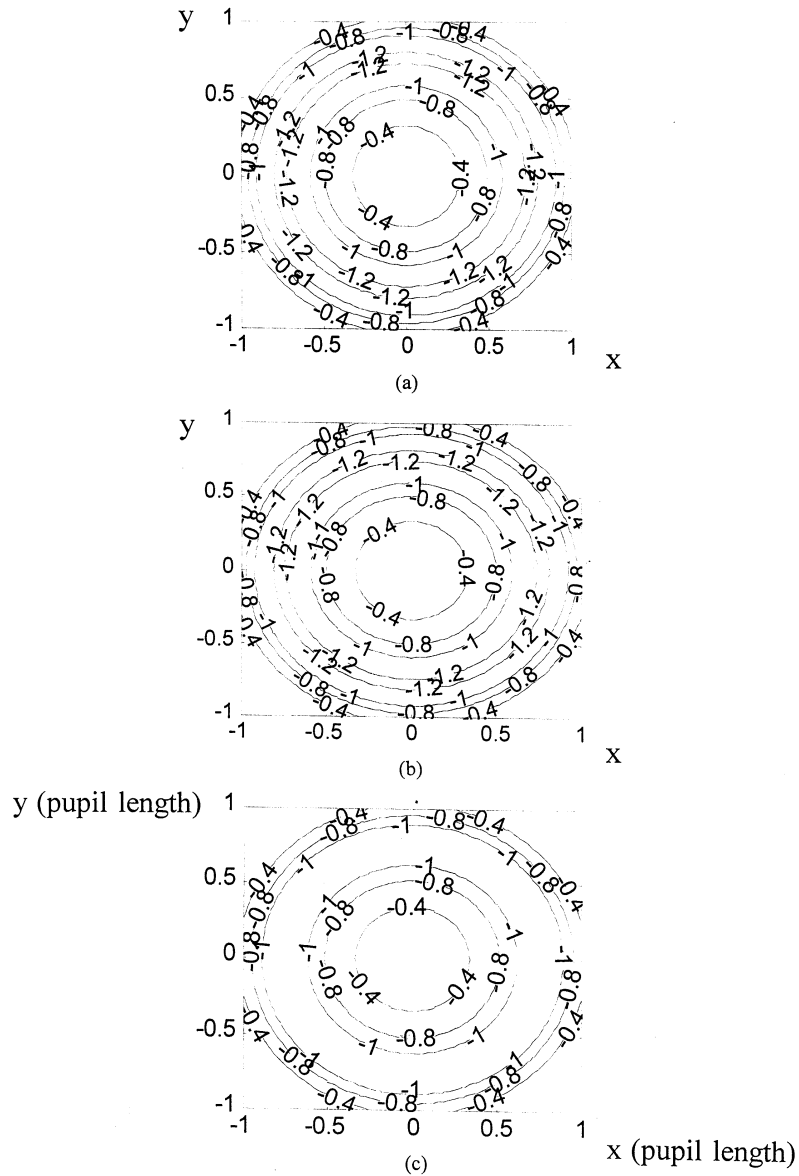


FIG. 3. The (a) contour of the original, (b) reconstructed by the WT method, and (c) by the LS method in a unit square exit pupil.

Here, E_S is the sum of squares of the data values in the original wave-front and E_N is the sum of squares of the random noise. The wave-fronts tested in our simulations were created by adding Gaussian white noises to the original wave-front. Table III shows the SNRs of the two algorithms for the test wave-fronts and Gaussian white noises. For further comparison, the SNR value as a function of the variance of the noise value was also investigated. Fig. 5 indicates that the WT method can provide a better SNR than the LS method.

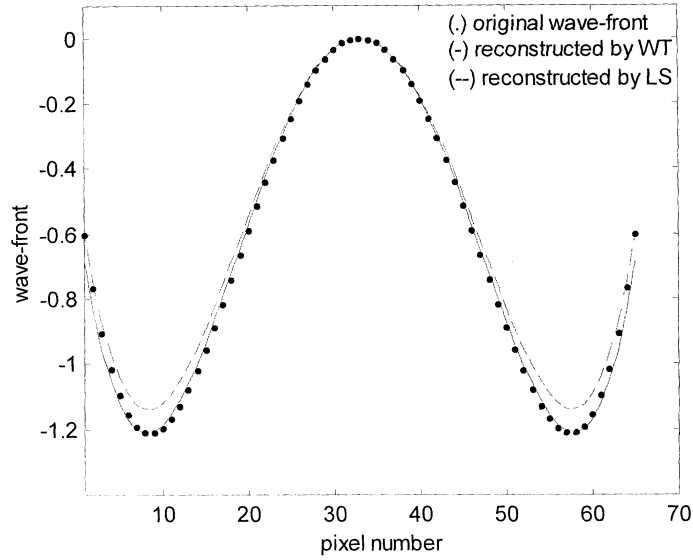


FIG. 4. Wave-fronts derived using the WT method (solid line), the LS method (dashed line), and the true wave function (dot line) of the axial case ($x = 0$).

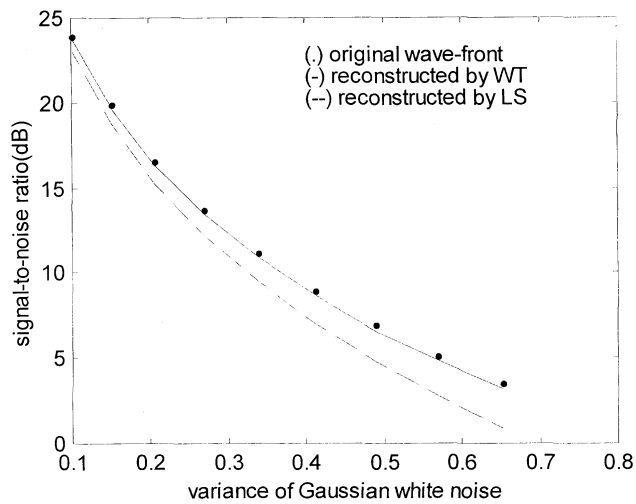


FIG. 5. The comparison of SNRs under input noise.

In summary, these simulation results indicate that the performance of the new algorithm is better than that of the LS method. In these simulations, all results were conducted by using Matlab version 5.2.0 [14].

TABLE III. SNRs of the different algorithms.

mean	Gaussian noise		SNRs of test wave fronts (dB)		
	variance		original	WT	LS
0	0.102		23.90	23.74	23.01
0	0.151		19.89	19.70	18.79
0	0.207		15.54	16.34	15.25
0	0.270		13.68	13.46	12.18
0	0.339		11.18	10.94	9.46
0	0.412		8.96	8.70	7.03
0	0.490		6.95	6.48	2.78
0	0.570		5.13	4.87	9.62
0	0.653		3.47	3.20	0.89

V. Conclusion

In this paper, a new technique for the direct evaluation of rotationally symmetric wave aberrations of an optical system is presented. The random noise has infinite extensions in space, but the wavelet transform localizes the signal in both the space and frequency domains. By varying its dilation parameter, this method evaluates the wave-front with a suitable filter (suitable dilation factor a) to obtain a unique value of the wave aberration coefficients. It is therefore immune to the noise and able to estimate the rotationally symmetric wave aberrations accurately. The WT method also provides a better SNR than the LS method. Using the SNR, we numerically demonstrate that the WT method can do a better job than the LS method.

This method also can be applied in other fields, such as interferogram reduction and aberration extraction in the Hartmann test. In future work, we are going to fit the primary (Seidel) aberration by using the two-dimensional discrete wavelet transform (DWT)

Acknowledgement

This work has been funded by National Science Council, Taiwan, R.O.C. under project grants NSC88-2215-E-008-008 and project NSC89-2215-E-008-010.

References

- [1] M. Born and E. Wolf, *Principles of Optics* (Pergamon, New York, 1975), Sec. 9.2.
- [2] F. Zernike, *Physica* **1**, 689 (1934).
- [3] D. Malacara, J. M. Carpio-Valadèz, and J. J. Sánchez-Mondragòn, *Opt. Eng.* **29**, 672 (1990).
- [4] J. Y. Wang and D. E. Silva, *Appl. Opt.* **19**, 1510 (1980).
- [5] E. Freysz, B. Pouligny, F. Argoul, and A. Arneodo, *Phys. Rev. Lett.* **64**, 7745 (1990).
- [6] R. K. Martinet, J. Morlet and A. Grossmann, *Int. J. Patt. Rec Art. Intell.* **1**, 273 (1987).

- [7] H. J. Caufield, *Photon. Spectra* **26**, 73 (1992).
- [8] J. M. Combes, A. Grossmann and Ph. Tchamitchian, in *Wavelets: Time-Frequency Methods and Phase Space* (Springer-Verlag, Berlin, 1989).
- [9] G. E. Forsythe, *J. Soc. Ind. Math.* **5**, 74 (1957).
- [10] Daubechies, *IEEE Trans. Inf. Theory* **36**, 961 (1990).
- [11] H. Szu, Y. Sheng and J. Chen, *Appl. Opt.* **31**, 3267 (1992).
- [12] Y. Sheng, D. Roberge and H. Szu, *Opt. Eng.* **31**, 1840 (1992).
- [13] D. Marr, E. Hildreth, *Proc. Royal Soc. London B* **207**, (1980).
- [14] *Wavelet Toolbox For Use with MATLAB* (The Math Works, Inc, Matick, 1997)